ISSN 1063-7761, Journal of Experimental and Theoretical Physics, 2022, Vol. 134, No. 4, pp. 506–510. © Pleiades Publishing, Inc., 2022.
Russian Text © The Author(s), 2022, published in Zhurnal Eksperimental'noi i Teoreticheskoi Fiziki, 2022, Vol. 161, No. 4, pp. 590–595.

This article was prepared for the special issue dedicated to the centenary of A. E. Chudakov

Muon Radiography of Large Natural and Industrial Objects—A New Stage in the Nuclear Emulsion Technique

A. B. Aleksandrov[a], S. G. Vasina[a,b], V. I. Galkin[c], V. M. Grachev[d], A. S. Konovalov[e], N. S. Konovalova[a], P. S. Korolev[f], A. A. Larionov[f], A. K. Managadze[g], I. A. Melnichenko[h], N. M. Okateva[a], N. G. Polukhina[a,d,h], T. M. Roganova[g], Zh. T. Sadykov[h], N. I. Starkov[a], E. N. Starkova[a], V. E. Tioukov[a], M. M. Chernyavskiy[a], V. I. Shevchenko[d], and T. V. Shchedrina[a,*]

[a] *Lebedev Physical Institute, Russian Academy of Sciences, Moscow, 119991 Russia*
[b] *Joint Institute for Nuclear Research, Dubna, Moscow Oblast, 141980 Russia*
[c] *Moscow State University, Moscow, 119991 Russia*
[d] *National Research Nuclear University MEPhI, Moscow, 115409 Russia*
[e] *Sergo Ordzhonikidze Russian State University for Geological Prospecting, Moscow, 117997 Russia*
[f] *Moscow Theological Academy of the Russian Orthodox Church, Sergiev Posad, Moscow oblast, 141300 Russia*
[g] *Skobeltsyn Research Institute of Nuclear Physics, Moscow University, Moscow, 119991 Russia*
[h] *National University of Science and Technology MISiS, Moscow, 119049 Russia*
**e-mail: tvshchedrina@gmail.com*

Received December 3, 2021; revised December 13, 2021; accepted December 13, 2021

Abstract—A new study of a historical object on the territory of the Russian Federation, the Holy Trinity Danilov Monastery, implemented by the muon radiography is presented. The method is based on the registration of changes in the cosmic muon fluxes during their passage through the object under study. Nuclear photoemulsions with unique spatial and angular resolution having the widest range of applications in experimental nuclear physics were used as experimental equipment. The experiment demonstrates a high efficiency of the method in the search for hidden objects, the presence of which on the territory of the monastery is confirmed by the results obtained.

DOI: 10.1134/S106377612204001X

INTRODUCTION

Track detectors of various types have been successfully used for a long time in the experimental nuclear physics and the elementary particle physics, which is related to their unique spatial resolution, the possibility of separating particle tracks, and the visualization and reliability of registering a spatial pattern of an interaction. In the development of nuclear physics, track detectors played an outstanding role, which is confirmed by a series of Nobel Prizes (1903, A. Becquerel; 1927, Ch. Wilson; 1936, W. Hess; 1950, S. W. Powell; 1960, D. Glaser; 1968, Alvarez; 1992, G. Charpak).

Owing to the simplicity of their design, track detectors have a very wide range of use: they are exposed at accelerators [1, 2], in the stratosphere [3, 4], under high-altitude conditions [5], and in underground low-background laboratories [6]. For example, track detectors based on nuclear photoemulsions were used to detect proton decay, double beta decay, and solar neutrino fluxes for the first time in deep underground laboratories. Among the discoveries in the field of cosmic ray physics made using nuclear photoemulsions, it is necessary to note the first experimental confirmations of the existence of a pion, an antiproton, and heavy mesons and the detection of nuclei heavier than a proton in cosmic rays [7, 8]. One of the most resonant experiments based on nuclear-emulsion track detectors was the discovery of a previously unknown large chamber in the body of the Pyramid of Cheops in 2016 [9]. The pyramid was subjected to muon radiography tests using relativistic cosmic muons.

With the help of nuclear photoemulsions, the effect of reducing ionization losses for narrow electron–positron pairs (so-called Chudakov effect); this effect which consists in the fact that the electromagnetic fields of the closely related components of a high-energy electron–positron pair (above several hundred GeV) partially compensate each other [10]. At such energies, the angle of separation of an electron and a positron is so low that the beginning of the traces of the pair in a photoemulsion looks like a track of a single particle with a reduced ionizing ability; that is, the ionization produced jointly by two relativistic charged particles turns out to be less than the minimum ionization caused by one of them.

Nuclear photoemulsion is one of the most popular track detectors at present. It consists of silver halide crystals uniformly distributed in a gelatin base. Each crystal acts as an independent charged particle detector, forming an ionization-induced latent image, which becomes visible under an optical microscope after chemical development [11]. The tracks of charged particles in a nuclear photoemulsion look like chains of developed grains, and the geometric parameters of a track depend on the charge and velocity of a detected particle. In experiments, this material is used in the form of emulsion films, where photoemulsion layers several tens of microns thick are poured on both sides to a thin synthetic base.

Nuclear emulsion detectors consist of stacks of double-sided emulsion films, the area of which is determined by the requirements of an experiment. At present, the only manufacturer of nuclear photoemulsions in Russia is OAO Slavich, which produces an emulsion gel and emulsion films, which meet the international quality requirements. Specialists at the Slavich enterprise in cooperation with the authors of the article are developing new types of photoemulsions with the widest range of parameters.

At the initial stage of the development of a nuclear emulsion technique, the ionization created by a charged particle in a photoemulsion was determined by photometry measurement of the blackening density of a trace. For this purpose, special devices, namely, photometers were created in order to determine the overall blackening of the trace [12–15]. The measured relative blackening and the length trace were used to determine the particle charge and velocity and, in combination with the residual range or multiple scattering, the particle mass [16].

Currently, the development of technologies for producing nuclear photoemulsions of various sensitivities and the progress in automated scanning equipment based on programmable microscopes [17, 18] allow us to approach the solution of such complex experimental problems as direct detection of dark matter particles [19].

The article gives an idea of the current state of the nuclear emulsion technique in Russia on the example of one of the muon radiography experiments carried out by the authors.

EXPERIMENTAL

The high intensity of the weakly interacting atmospheric muon fluxes with a high penetrability near the Earth's surface makes it possible to study large natural and industrial objects by muon radiography and to take 3D images of their internal structure, similarly to an X-ray image [20]. Passing through regions with different matter densities and undergoing different degrees of absorption, charged muon fluxes carry information about the features of the internal structure of the objects they passed through. Anomalies in the angular distributions of the registered particle tracks may indicate the presence in a certain direction of areas that differ in density from the main substance (i.e., voids or foreign inclusions) in a certain direction. To obtain this information, it is sufficient to have a detector to detect the angular distribution of charged particles over a wide angular range.

For several years, the authors have been conducting research using muon radiography and nuclear emulsion detectors to study historical monuments in Russia [21, 22]. Currently, an experiment is being carried out to search for hidden underground premises and fragments of buildings of the Holy Trinity Danilov Monastery in Pereslavl-Zalessky, Yaroslavl region [23].

According to the experimental technique, nuclear photoemulsion layers packed in light-tight bags are fixed in a vertical position with metal structures developed at the National University of Science and Technology MISiS (Fig. 1). Shown in Fig. 1 detector consisted of 4 emulsion modules 10×12.5 cm^2 in size, 5 layers each, total filling of one detector was 20 emulsion layers. The stacks of the nuclear photoemulsion layers detect the tracks of incident atmospheric muons, which allow us to compare the particle fluxes coming from different directions and to determine their angular characteristics. The spatial resolution of the two-sided photoemulsion during the restoration of a muon track is 2–3 μm and the angular resolution is about 1 msr.

The publication presents the latest results of probing some areas in the underground space of the monastery in the vicinity of the Church of All Saints (Fig. 2a). Figure 2b shows the installation scheme of nuclear emulsion detectors D11, D12, D13, and D18 in the basement of the church.

The detectors are directed to see the old foundation (D11, D12), if it was and has been preserved, and to see the territory between churches *1* and *3* (D13, D18), i.e., possible burials and the remains of the underground passage used earlier for heating the Church of All Saints.

As the experiments in [24, 25] showed, the exposure time of the detectors should be at least two months in order to obtain statistically reliable angular distributions under the observation conditions. After the end of the exposure, the detectors are dismantled and the nuclear photoemulsion is subjected to a devel-

Fig. 1. Nuclear-photoemulsion detectors placed in the basement of on ethe churches of the Holy Trinity Danilov Monastery.

opment procedure in the chemical laboratory of OAO Slavich. The scanning of the developed films, the measurement of particle track parameters, and primary data analysis were carried out using an automated microscope, which is part of the multifunctional PAVICOM complex for processing track detector data [26]. Further analysis uses the measured angular characteristics of tracks t_x and t_y associated with angles φ and θ of particle trajectories relative to the normal to the detector plane,

$$t_x = \frac{dx}{dz} = \tan\theta\cos\varphi,$$

$$t_y = \frac{dy}{dz} = \tan\theta\sin\varphi.$$

RESULTS AND DISCUSSION

Detectors D13 and D18 were installed sequentially in the basement of the building of the Church of All Saints and had the same exposure time of about 2.5 months. Both detectors were located approximately in the same place, and the scheme of their location is shown schematically in Fig. 2b. Since both detectors were used for an experimental study of the same object under identical conditions, structural features in the data obtained by both detectors reflect the real structures of the object under study. Figure 3 shows the reconstructed data of detectors D13 and D18 in the form of the distribution of the number of muons in variables t_x and t_y.

The main part of the broad peaks at $t_x = 0$, $t_y = \pm 0.5$ corresponds to the natural distribution of muon fluxes in the given angular ranges

($\theta < 45°$). However, the following additional local maxima are detected against this background (their positions are indicated by numerals *1*, *2*, *3* in Fig. 3):

(1) inhomogeneity in the "backward" direction at $t_y = 0.45$, $t_x = -0.1$,

(2) inhomogeneity in the "forward" direction at $t_y = -0.5$, $t_x = 0.18$, and

(3) wide inhomogeneity in the forward direction at $t_y = -0.5$, t_x from –0.2 to 0.1.

The presence of these maxima indicates the presence of areas with a lower absorption capacity in these directions. Taking into account the fact that the values of the variable $t_y = \pm 0.5$ correspond to an angle of 20°–25° to the horizon, these features are located at a distance of no more than 7–8 m horizontally from the detector position.

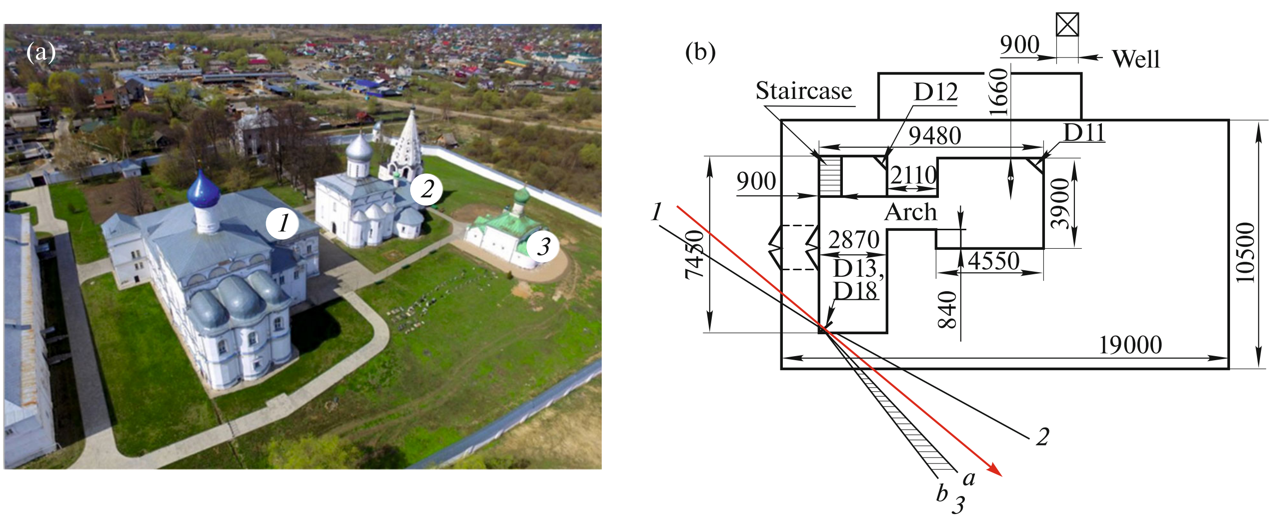

Fig. 2. (a) Temple complex of the monastery ((*1*) Church of the Praise of the Mother of God, (*2*) Cathedral of the Holy Trinity with the Church of St. Daniel, (*3*) Church of All Saints). (b) Location of detectors D11, D12, D13, and D18 in the basement of the Church of All Saints. Directions *1*, *2*, and *3* indicate the directions of the features of muon fluxes detected and discussed in this work.

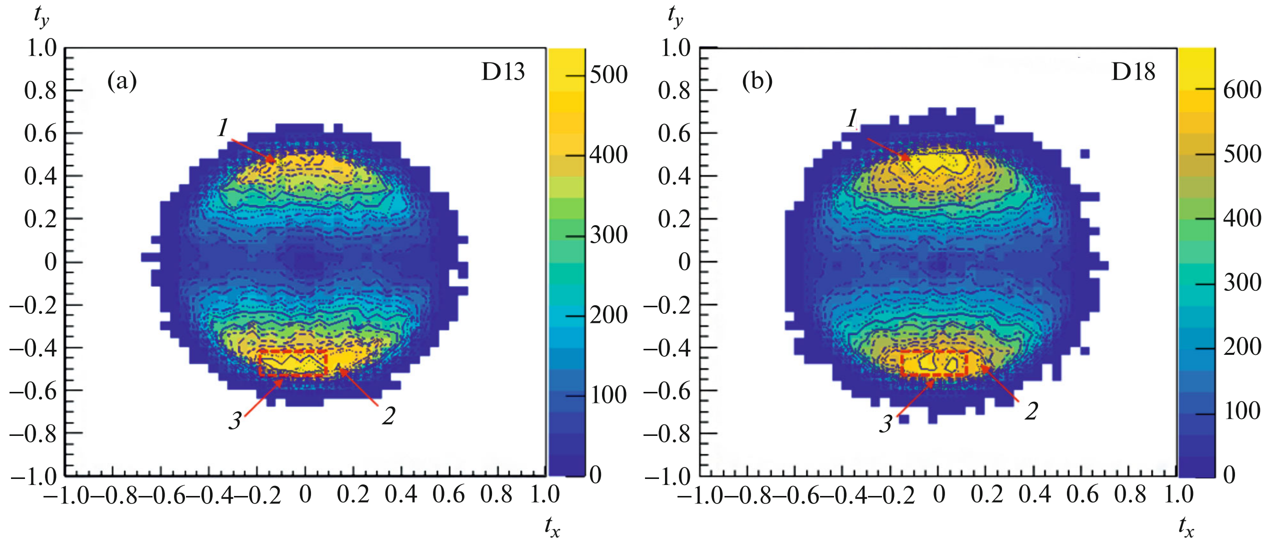

Fig. 3. Angular distributions of the experimental data obtained by detectors (a) D13 and (b) D18 in building 3. The color scale on the histogram indicates the number of detected muons per bin unit. Along the ordinate axis, $t_y > 0$ corresponds to the "backward" direction (upper hemisphere) and $t_y < 0$, to the "forward" direction.

Below we discuss each of the detected features.

Maximum number *1* in the "backward" direction can correspond to a small object, i.e., a cavity or region with a density lower than that of the base material (ground, walls, etc.).

At a high probability, maximum number *2* in the "forward" direction most likely corresponds to the doorway that leads into the cell between the basement and the first floor.

The regions near $t_x = 0$ correspond to the natural maximum of the muon flux at a fixed t_y and, in a first approximation, should be the same in the forward and backward directions. However, a wide inhomogeneity (indicated by number *3*) much exceeding the natural background is visible in the forward direction at $t_y = -0.5$. Its large angular size can reflect large linear dimensions, which depend on the distance from the detector and can be estimated from sector *a*–*b* in Fig. 2b.

Taking into account an angle of 20°–25° to the horizon, the visibility radius of the detector is 6–8 m. For convenience, Fig. 4 shows the terrain map and the directions of structural features *1*, *2*, and *3* and the field of visibility in the form of a circle at a basement depth of 3 m relative to the ground level.

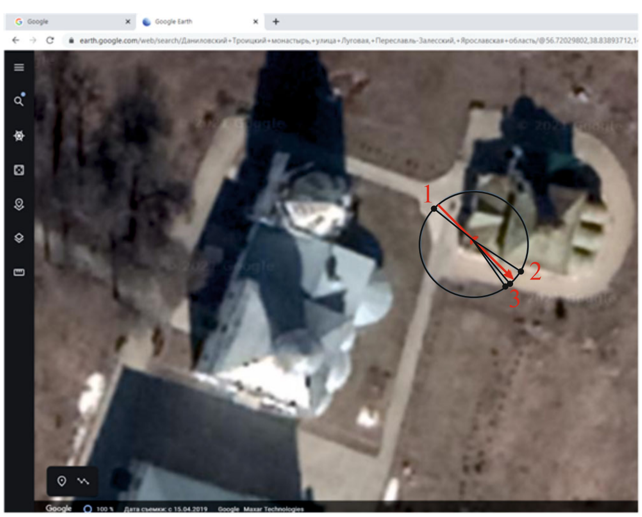

Fig. 4. Terrain map made using a GooglePro photograph. The circle indicates the visibility radius of the detector, and numerals *1*, *2*, and *3* indicate the directions of the detected structural features in the experimental angular distribution of muons.

CONCLUSIONS

The experiments conducted at the Holy Trinity Danilov Monastery demonstrate that the muon radiography method based on emulsion track detectors is a promising alternative method for probing of large-scale geological and industrial objects. Emulsion detectors have a number of undeniable advantages, including a high spatial (less than 1 μm) and angular (about 1 msr) resolution, large information capacity, small sizes (1 m^2 or less), ease of transportation, and ease of operation under difficult conditions.

The muon radiography method based on the emulsion track detectors enables to diagnose a wide variety of natural and industrial objects using economical and compact detectors of a fairly simple design, which distinguishes it from more expensive alternative methods. The increased interest in muon radiography is determined by the rapid development of precision scanning equipment, which allows one to process large relativistic emulsion areas in a relatively short time.

Our methodological approaches and prototypes of technical solutions presented in this work for the implementation of muon radiography using emulsion track detectors for studying the state of a UNESCO cultural heritage site and our analysis of experimental results are of great importance for the further prospects for the implementation of muon radiography in Russia.

CONFLICT OF INTEREST

The authors declare that they have no conflicts of interest.

REFERENCES

1. T. Nakamura, A. Ariga, T. Ban, et al., Nucl. Instrum. Methods Phys. Res., Sect. A **556**, 80 (2006).
2. C. Ahdida, R. Albanese, A. Alexandrov, et al., J. Instrum. **14**, P03025 (2019).
3. N. A. Dobrotin, K. A. Kotel'nikov, A. V. Apanasenko, et al., Izv. Akad. Nauk SSSR, Ser. Fiz. **53**, 250 (1989).
4. G. T. Zatsepin, S. I. Nikol'skii, I. V. Rakobol'skaya, et al., Izv. Akad. Nauk SSSR, Ser. Fiz. **61**, 1186 (1997).
5. V. Tioukov, A. Alexandrov, C. Bozza, et al., Sci. Rep. **9**, 6695 (2019).
6. N. Agafonova, A. Aleksandrov, A. Anokhina, et al., J. Phys.: Conf. Ser. **869**, 012048 (2017).
7. C. F. Powell, P. H. Fowler, and D. H. Perkins, *Study of Elementary Particles by the Photographic Method* (Pergamon, Oxford, 1959).
8. D. H. Perkins, *Introduction to High Energy Physics* (Cambridge Univ. Press, Cambridge, 2000).
9. K. Morishima, M. Kuno, A. Nishio, et al., Nature (London, U.K.) **552**, 386 (2017).
10. A. E. Chudakov, Izv. Akad. Nauk SSSR, Ser. Fiz. **19**, 651 (1955).
11. A. Ariga, T. Ariga, G. de Lellis, et al., in *Particle Physics Reference Library*, Vol. 2: *Detectors for Particles and Radiations* (Springer, Cham, 2020), p. 383.
12. S. Friesen and K. Kristiansson, Nature (London, U.K.) **16**, 686 (1950).
13. K. Kristiansson, Philos. Mag. **44**, 268 (1953).
14. S. Friesen and L. Stigmark, Ark. Fysik **8**, 121 (1954).
15. S. Friesen, Ark. Fysik **8**, 305 (1953).
16. B. A. Voikovskii, A. I. Galaktionov, M. I. Tret'yakova, et al., Prib. Tekh. Eksp., No. 6, 38 (1957).
17. A. Alexandrov, A. Buonaura, L. Consiglio, et al., J. Instrum. **11**, P06002 (2016).
18. A. Alexandrov, G. de Lellis, and V. Tioukov, Sci. Rep. **9** (2019).
19. N. Agafonova, A. Aleksandrov, A. Anokhina, et al., Eur. Phys. J. C **78**, 578 (2018).
20. A. B. Alexandrov, M. S. Vladimirov, V. I. Galkin, L. A. Goncharova, V. M. Grachev, S. G. Vasina, N. S. Konovalova, A. A. Malovichko, A. K. Managadze, N. M. Okat'eva, N. G. Polukhina, T. M. Roganova, N. I. Starkov, V. E. Tioukov, M. M. Chernyavsky, and T. V. Shchedrina, Phys. Usp. **60**, 1277 (2017).
21. S. A. Baklagin, V. M. Grachev, N. S. Konovalova, et al., Int. J. Innov. Res. Sci. Eng. Technol. **5**, 0507027 (2016).
22. A. Abiev, A. Bagulya, M. Chernyavsky, et al., Appl. Sci. **9**, 2040 (2019).
23. A. B. Aleksandrov, S. G. Vasina, V. I. Galkin, L. A. Goncharova, A. S. Konovalov, N. S. Konovalova, P. S. Korolev, A. A. Larionov, I. A. Melnichenko, A. K. Managadze, N. M. Okateva, N. G. Polukhina, T. M. Roganova, Zh. T. Sadykov, N. I. Starkov, et al., Phys. At. Nucl. **84**, 855 (2021).
24. A. B. Aleksandrov, A. V. Bagulya, M. S. Vladimirov, M. M. Chernyavsky, V. I. Galkin, L. G. Dedenko, N. V. Fomenko, N. S. Konovalova, G. de Lellis, A. K. Managadze, O. I. Orurk, N. G. Polukhina, T. M. Roganova, T. V. Shchedrina, C. Sirignano, N. I. Starkov, et al., Phys. Part. Nucl. Lett. **12**, 713 (2015).
25. A. B. Aleksandrov, A. V. Bagulya, M. M. Chernyavsky, et al., AIP Conf. Proc. **1702**, 110002 (2015).
26. A. Alexandrov, N. Konovalova, N. Okateva, et al., Measurement **187**, 110244 (2022).

Translated by K. Shakhlevich